FINAL PUBLISHABLE REPORT

Grant Agreement number	18SIB09
Project short name	TEMMT
Project full title	Traceability of electrical measurements at millimetre-wave and terahertz frequencies for communications and electronics technologies

Project start date and duration:	1st May 2019, 39 months	
Coordinator: Xiaobang Shang, NPL Tel: +44 208 943 6643 E-mail: xiaobang.shang@npl.co.uk Project website address: http://projects.lne.eu/jrp-temmt/		
1. NPL, United Kingdom 2. CMI, Czech Republic 3. GUM, Poland 4. LNE, France 5. METAS, Switzerland 6. PTB, Germany 7. TUBITAK, Turkey 8. VSL, Netherlands	9. BHAM, United Kingdom 10. Chalmers, Sweden 11. FVB, Germany (withdrawn from January 2021) 12. ULILLE, France 13. WAT, Poland 14. FBH, Germany (joined January 2021, follow-up for FVB)	15. Anritsu, United Kingdom 16. FormFactor, Germany 17. INTI, Argentina 18. Keysight BE, Belgium 19. R&S, Germany 20. VDI, United States
RMG -		

TABLE OF CONTENTS

1 Overview

This project aimed to establish traceability to the SI for 3 electrical measurement quantities: (i) S-parameters, (ii) power and (iii) complex permittivity of dielectric materials, at millimetre-wave and terahertz (THz) frequencies. As a result of this project, measurement capability has now been put in place, across several European NMIs, for accurate and traceable measurements of these 3 parameters at the millimetre-wave and THz frequencies. The capability provides direct benefits to applications that utilize this part of the spectrum, including point-to-point backhaul for 5G communications and beyond, the Internet of Things (IoT), radar sensors for connected and autonomous vehicles (CAVs), space-borne radiometers for remote sensing of the Earth and security imaging. Outputs of this project enable end-users to have confidence in measurement and specifications and to offer assured products through measurement traceability chains.

2 Need

The rollout of 5G networks and large-scale deployments of cellular IoT will lead to fundamental changes to our society, impacting not only consumer services but also industries embarking on digital transformations. CAVs are progressing rapidly and are expected to improve traffic flow, safety and convenience significantly. Space deployed radiometers are used for passive remote sensing of atmospheric constituents which are related to climate change and play a critical role in environmental protection. All these applications require the use of the millimetre-wave and THz regions of the electromagnetic spectrum, and demand devices and integrated circuits operating at these high frequencies.

However, the development of devices and systems to underpin these applications is currently hampered by the lack of traceability for electrical measurements at millimetre-wave and THz frequencies. For example, although power meters working at frequencies up to at least 750 GHz are commercially available, there is no established calibration hierarchy, accessible to industrial and other end-users, to allow traceability to the SI for these measurements. In addition, current commercially available frequency extender heads and calibration kits for vector network analysers (VNAs) enable these systems to measure S-parameters at frequencies up to 1.5 THz. These VNA systems can also be adapted to measure materials properties (e.g. complex permittivity) using commercially available Material Characterisation Kits (MCK) at frequencies up to at least 750 GHz. However, again, there is no traceability to the SI to benchmark this measurement capability. NMI-level metrology research is therefore, urgently needed to address this lack of traceability so that the capabilities of these high frequency measurement systems can be fully exploited.

This is important to ensure product quality and end user confidence, and ultimately to improve the competitiveness of European Industry. The work in this project also aligns with broader European visions, as outlined in the Europe Commission Strategy i.e. “Digital Single Market”.

3 Objectives

The overall objective of this project is to achieve accurate and traceable electrical measurements for users of the millimetre-wave and THz regions of the electromagnetic spectrum, particularly for electronics applications impacting future communications technologies – so-called 5G communications and beyond.

The specific objectives of the project are:

1. To develop metrological traceability and verification techniques for S-parameters (that measure the loss and phase change for transmitted and reflected signals) in both coaxial line (using the 1.35 mm E-band connector to 90 GHz) and rectangular metallic waveguide (using waveguides covering frequencies from 330 GHz to 1.5 THz). Three waveguide bands within this frequency range will be covered and these are 330 GHz to 500 GHz, 500 GHz to 750 GHz, and 1.1 THz to 1.5 THz.
2. To develop metrological traceability and verification techniques for S-parameter measurements on planar substrates from 110 GHz to 1.1 THz. Three waveguide bands within this frequency range will be covered and these are 110 GHz to 170 GHz, 500 GHz to 750 GHz, and 750 GHz to 1.1 THz.
3. To develop metrological traceability for power measurements in waveguide to 750 GHz. Two waveguide bands within this frequency range will be covered and these are 110 GHz to 170 GHz, and 500 GHz to 750 GHz.

4. To develop metrological traceability for complex permittivity of dielectric materials to 750 GHz. Two waveguide bands will be covered and these are 140 GHz to 220 GHz, and 500 GHz to 750 GHz.
5. To facilitate the take up of the technology and measurement infrastructure developed in the project by other NMIs with the view of forming a coordinated network of NMIs that provide a comprehensive measurement capability as well as by the measurement supply chain (research institutes, calibration laboratories), standards developing organisations (e.g. IEEE P287 and IEEE P1785) and end users (i.e. manufacturers of telecom equipment, measuring instruments, absorber materials, etc).

4 Results

4.1 Objective 1: To develop metrological traceability and verification techniques for S-parameters (that measure the loss and phase change for transmitted and reflected signals) in both coaxial line (using the 1.35 mm E-band connector to 90 GHz) and rectangular metallic waveguide (using waveguides covering frequencies from 330 GHz to 1.5 THz). Three waveguide bands within this frequency range will be covered and these are 330 GHz to 500 GHz, 500 GHz to 750 GHz, and 1.1 THz to 1.5 THz.

Work on the "Traceable connectorised S-parameter measurements" had an overall objective to develop and establish metrological traceability and verification techniques for S-parameters in both coaxial line and rectangular metallic waveguide. Work on the "Coaxial dimensional traceability" and "Coaxial electrical traceability" were focused on establishing traceability in the 1.35 mm E-band connector which operates up to 90 GHz. Work has been also undertaken on the "Waveguide electrical traceability", focusing on establishing traceability in three waveguide bands: 330-500 GHz, 500-750 GHz, and 1.1-1.5 THz.

4.1.1 Coaxial line traceability

The objective of this study was to establish NMI-level measurement capabilities for the determination of conductor dimensional properties such as the inner conductor outer diameters (ICOD) and the outer conductor inner diameters (OCID) for 1.35 mm coaxial air-lines, including the derivation of uncertainties associated with such systems. For example, the measurement system developed by LNE comprised a combination of air-gauging and laser micrometer techniques. This is shown in Figure 1.1. The system developed by INTI was based around a scanning electron microscope, as shown in Figure 1.2. An output from this study was an interlaboratory measurement comparison exercise where each participant (NPL, LNE, PTB and INTI, as well as a contribution from another consortium member, TUBITAK-UME) utilised the systems they developed in this study to measure a set of travelling standards.

Although not a named partner in this study, an additional member of the consortium, TUBITAK-UME from Türkiye (formally Turkey), contributed to the measurement comparison activity. TUBITAK-UME used an automated in-house diameter measurement system capable of ICOD and OCID measurements. The OCID was measured using an air gauge system and the ICOD was measured using a laser scanner. The connector details (chamfers, pins, holes, etc) were measured using an optical method.

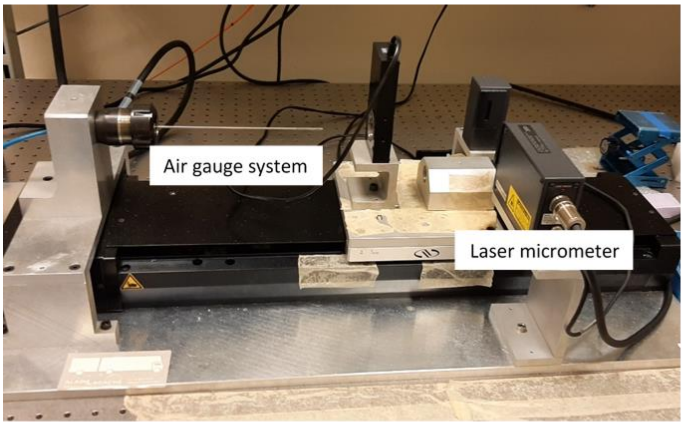

Fig 1.1: LNE air-line dimensional measurement system.

Fig 1.2: INTI Scanning Electron Microscope (left) and a reference standard image (right)

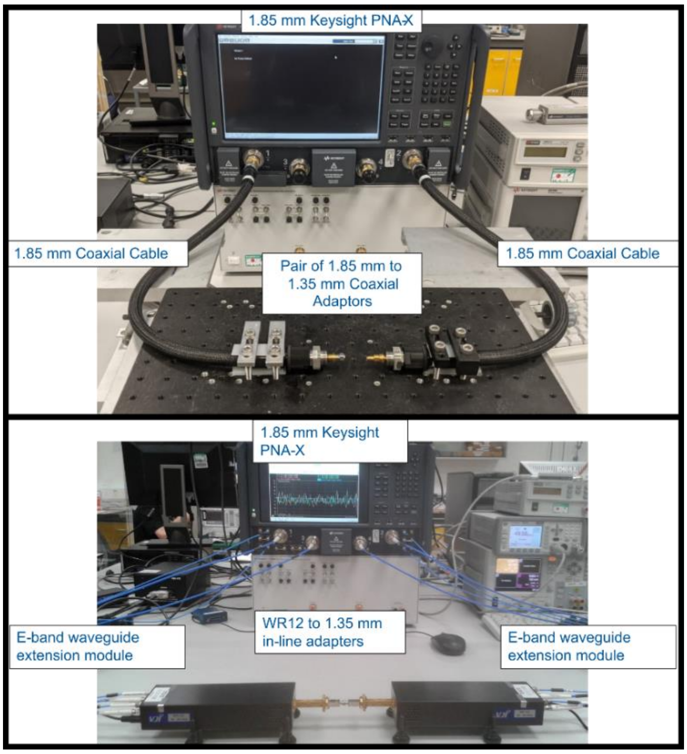

Fig 1.3: NPL's measurement setup for 1.35 mm coaxial line using: (i) V-band coaxial adaptors up to 67 GHz (top); and (ii) WR-12 waveguide adaptors up to 90 GHz (bottom).

Following work was carried out on establishing electrical measurement systems and associated uncertainties, with input from previous results regarding dimensional traceability for the electrical measurements. Partners involved on this were: NPL, LNE and PTB, with an output being an electrical measurement comparison up to 90 GHz using the systems established in this study. For example, the measurement system developed by NPL uses both coaxial adaptors (from V-connector to E-connector) to 67 GHz and waveguide adaptors (from WR-12 to E-connector) to measure up to 90 GHz. This is shown in Figure 1.3. The system developed by PTB is also comprised of two different setups: (i) 10 MHz to 70 GHz; (ii) 52.2 GHz to 98.5 GHz. Figure 1.4 shows the low band system, which operates to 70 GHz.

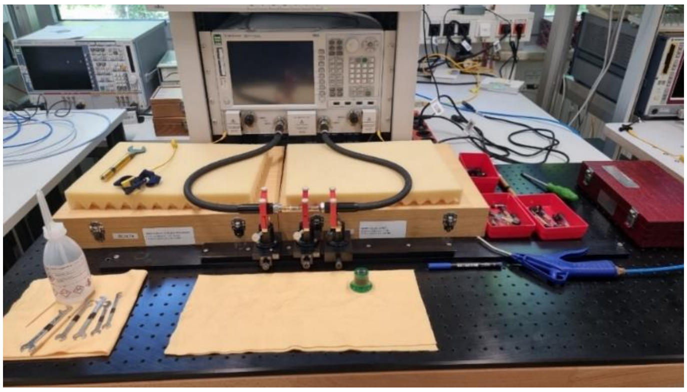

Fig 1.4: Measurement setup at PTB for the 10 MHz to 70 GHz frequency band with V-band connectors.

Below is a summary of the different systems established by each partner on dimensional traceability (Table 1.1) and electrical traceability (Table 1.2).

Table 1.1: Summary of dimensional measurement systems and capabilities developed by each project partner for the 1.35 mm coaxial line size

Partner	Measurand	System type	Typical uncertainties (µm)
NPL	OCID	Air plug gauge & manual translation stage	1.5
	ICOD	Laser micrometer & manual translation stage	1.5
LNE	OCID	Air plug gauge & automated translation stage	1.0
	ICOD	Laser micrometer & automated translation stage	0.5
PTB	OCID	Air plug gauge & automated vertical translation stage	2.0
	ICOD	LED-µm & automated translation stage	1.0
INTI	ICOD	Scanning electron microscope (SEM)	< 1.0
TUBITAK-UME	OCID	Automated Air Gauge system	1.3
	ICOD	Laser scanner	2.0

Table 1.2: Summary of electrical measurement systems and calibration techniques developed by each project partner for the 1.35 mm coaxial line size

Partner	Frequency range (GHz)	Types of standards	Type of calibration scheme
NPL	0.01 – 67	Short, Line, Through	Optimized mTRL

	60 – 90		
LNE	0.05 – 67	Short, Open, Load, Through	SOLT
	67 - 90		
PTB	0.01 – 70	Primary: Multiple offset shorts	Primary: SOOT
	52.2 – 98.5	Secondary: Short, Open, Load, Through	Secondary: Overdetermined SOLT

4.1.2 Waveguide traceability

The objective of this study was to establish S-parameter measurement capabilities for one- and two-port waveguide devices in three waveguide bands: (i) WM-570 (330-500 GHz); (ii) WM-380 (500-750 GHz); (iii) WM-164 (1.1-1.5 THz). The primary output was new measurement capabilities for each participant involved (i.e., NPL, University of Birmingham, VDI, Chalmers University of Technology and Anritsu).

For example, the measurement systems developed by the University of Birmingham, comprising a VNA and multiple pairs of frequency extender heads, is shown in Figure 1.5. The system developed by Chalmers is shown in Figure 1.6. Figure 1.7 shows some of the primary reference standards designed by NPL and used with these VNA systems. These standards were used to implement the ¾-wave Thru-Reflect-Line (TRL) calibration technique in these waveguide bands [1]. Traceability is established in these waveguide bands using the techniques described in [2].

Fig 1.5: Waveguide *S*-parameter measurement set-up at the University of Birmingham.

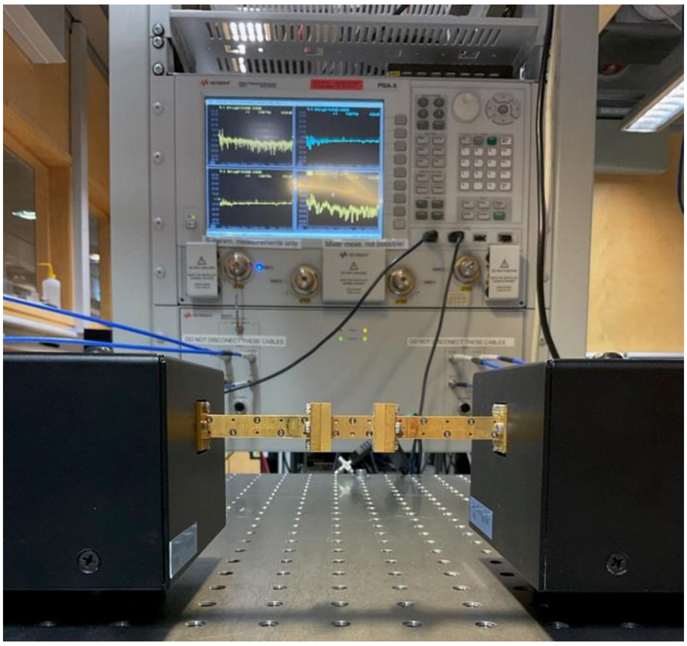

Fig 1.6: Waveguide S-parameter measurement set-up at Chalmers University of Technology.

Fig 1.7: NPL's primary reference standards for WM-380 waveguide measurements (500 – 750 GHz).

Table 1.3 gives a summary of the new waveguide measurement capabilities that have been established by each participant in this project.

Table 1.3: Waveguide measurement capabilities developed by the partners involved

Institute	Waveguide size	Frequency Range (GHz)	Types of Standards	Types of calibration
NPL	WM-570	330 – 500	Thru, Short 2 Lines (651 μm and 951 μm)	¾-wave TRL
	WM-380	500 – 750	Thru, Short 2 Lines (431 μm and 568 μm)	¾-wave TRL
BHAM	WM-570	330 – 500	Short, Offset short Load, Thru	SOLT
	WM-380	500 – 750	Short, Offset short Load, Thru	SOLT
VDI	WM-570	330 – 500	Short, Offset short Load, Thru	SOLT
	WM-380	500 – 750	Thru, Line Short	¼-wave TRL
	WM-164	1100 – 1500	Short, Offset short Load, Thru	SOLT
Chalmers	WM-380	500 – 750	Short, Offset short Load, Thru	SOLT
	WM-164	1100 – 1500	Short, Offset short Load, Thru	SOLT
Anritsu	WM-570	330 – 500	Thru, Line Short, Offset short 1, Offset short 2 Load	TRL SSLT MSSS

4.1.3 Summary

Partner laboratories have successfully established new measurement capabilities for the 1.35 mm (E-band) coaxial line size and three submillimetre-wave waveguide bands (WM-570, WM-380 and WM-164). For the coaxial line work, four partner laboratories have established new systems for the measurement of the dimensional properties of air-lines and three partner laboratories have established electrical (S-parameter) measurement systems. For the waveguide activities, five partner organisations have established new systems for electrical (S-parameter) measurements from 330 GHz to 1.5 THz.

For both the coaxial and waveguide measurement systems, performance has been validated through interlaboratory measurement comparisons for each of the relevant measurands. The establishment of these new measurement systems has significantly enhanced the metrological traceability currently in place across Europe for both coaxial lines and waveguides. Therefore, objective 1 has been successfully accomplished.

References

[1] N M Ridler, R G Clarke, C Li and M J Salter, “Strategies for Traceable Submillimeter-wave Vector Network Analyzer Measurements”, IEEE Trans Terahertz Science & Technology, Vol 9, No 4, pp 392-398, July 2019.

[2] N M Ridler, S Johny, M J Salter, X Shang, W Sun and A Wilson, “Establishing waveguide lines as primary standards for scattering parameter measurements at submillimetre wavelengths”, Metrologia, Vol 58, No 1, 015015, February 2021.

4.2 Objective 2: To develop metrological traceability and verification techniques for S-parameter measurements on planar substrates from 110 GHz to 1.1 THz. Three waveguide bands within this frequency range will be covered and these are 110 GHz to 170 GHz, 500 GHz to 750 GHz, and 750 GHz to 1.1 THz.

The technology is advancing rapidly for monolithic millimetre-wave integrated circuits (MMICs), with applications being developed at frequencies of hundreds of gigahertz. However, the development of such integrated circuits is hampered by the lack of traceability for on-wafer S-parameter measurements at these frequencies. There is a strong demand from stakeholders, in particular from the compound semiconductor industry, for traceable on-wafer measurements. Another EMPIR project, 14IND02 PlanarCal, performed preliminary studies into on-wafer measurements up to 220 GHz and beyond. Work was also successfully undertaken to establish the traceability of planar measurements up to 110 GHz. However, the project concluded that a significant new research effort was needed to establish traceability for on-wafer measurements above 110 GHz.

This project aimed to establish traceable on-wafer Coplanar Waveguide (CPW) S-parameter measurements up to 1.1 THz. First, a dedicated reference wafer was developed for calibration and validation up to 1.1 THz. Methods were developed for the assessment of uncertainty corresponding to each CPW standard. In addition, on-wafer calibration and verification techniques were investigated for application at frequencies exceeding 110 GHz. Subsequently, a study into sources of measurement uncertainties for on-wafer measurements led to a detailed list of uncertainty sources. Then, methods were developed for estimating the uncertainty sources needed for DUT uncertainty assessment. Also, measurement models were investigated for uncertainty propagation for on-wafer calibrations. Furthermore, methods for autonomous probing were developed to support accurate on-wafer measurements. Finally, the project completed a first-of-a-kind international interlaboratory comparison in on-wafer Coplanar Waveguide (CPW) measurements up to 1.1 THz.

4.2.1 Reference calibration substrates

To establish traceability and high accuracy for on-wafer S-parameter measurements, the calibration and validation devices were designed using the same technology: coplanar waveguide (CPW) based structures implemented on a high resistivity silicon (HR Si) wafer. LNE and FVB/FBH led the design of the reference wafer with support from other activity partners. Identical access structures were included in the design of all calibration and DUT structures to allow for an accurate definition of the measurement and reference planes and to realize consistent and accurate measurement results. The reference substrate includes calibration and verification kits that have been designed to cover the frequency range between 110 GHz and 1100 GHz. It includes a low-frequency set of standards operating from 110 GHz to 330 GHz and a high-frequency set operating from 330 GHz to 1100 GHz. The high-frequency standards were designed with smaller dimensions than the low-frequency standards in terms of cross-section and length. For instance, each set includes several transmission lines to allow broadband TRL calibration, with lengths ranging between 500 µm and 4280 µm for the low-frequency standards and between 120 µm and 1320 µm for the high-frequency standards. Besides transmission lines, the calibration kits include several offset shorts, opens, matched loads and fixed-distanced two-port structures embedding two one-port standards. The structures allow a range of different calibration techniques to be implemented, i.e. Thru-Reflect-Line (TRL), multiline TRL, and 16-term calibrations.

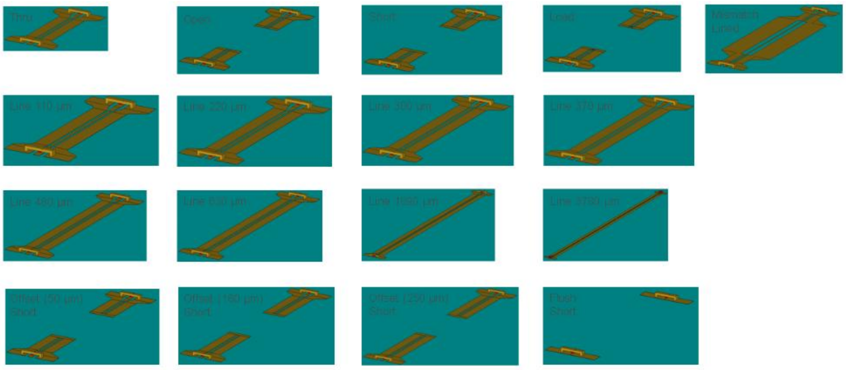

Fig 2.1: 3D models of 17 devices from Kit 1 for on-wafer CPW calibration and verification up to 330 GHz.

FVB/FBH employed electromagnetic field simulations to validate the calibration and validation standards. For each of the two kits, i.e. Kit 1 (110 GHz – 330 GHz) and Kit 2 (330 GHz – 1100 GHz), 17 structures were created based on the geometrical specifications provided by LNE. The calibration structures of Kit 1 are depicted in Figure 2.1 as an example. The structures related to Kit 2 are similar but are not shown for the sake of brevity. To reduce the computational expenses of EM simulations, each calibration structure was excited with the so-called bridge model rather than a sophisticated probe model, as seen in Figure 2.1. All 34 calibration structures of both kits were discretized using a hexahedral mesh. Thereafter, the transient solver of CST Studio Suite was used to compute the 2 x 2 complex-valued scattering matrices for each segment on the respective frequency interval.

The fabrication and parameterization of the reference substrate were performed by ULILLE. Two wafers, including eight identical calibration substrates, were produced. The microfabrication process was carried out using a 3-inch (76.2 +/- 0.3 mm) semi-insulating high resistivity (>5000 Ω.cm) Silicon (Si) wafer purchased from Siltronix®, with 275µm (+/-15 µm) thickness. After fabrication, a white-light interferometer was used for the determination of Ti and Ti/au thicknesses of the resistive and conductive layers respectively. The sheet resistance was measured using a standard four-point measurement technique. A TescanTM Mira XMU scanning electron microscope (SEM) was used to measure the critical dimensional parameters. In particular, 15 elements for each reference kit were captured, and images were processed offline to limit electron charging by the SEM, as shown in Figure 2.2.

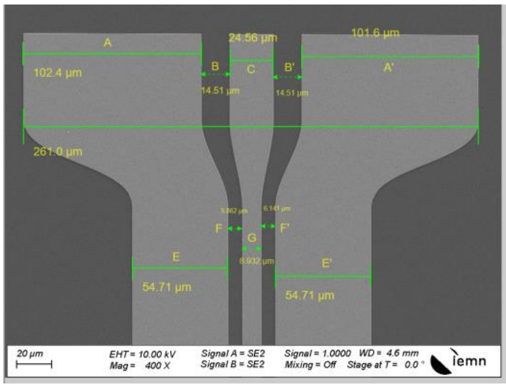

(a)

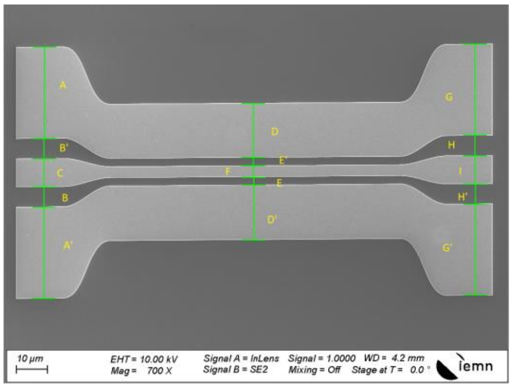

(b)

Fig 2.2: SEM images of (a) tapered section of a CPW structure and (b) CPW transmission line.

VSL led the development of the behaviour models of CPW devices incorporated on the reference calibration substrate to establish traceability for planar S-parameter measurements up to 1.1 THz. Detailed behaviour models designed in CST Microwave Studio software allowed the calculation of reference values and corresponding uncertainties. The frequency range of interest was 10 GHz to 1100 GHz. The purpose of the simulations was to identify all relevant parameters affecting the electrical behaviour of on-wafer CPW devices, thus recognizing and quantifying the uncertainty of each CPW device, as shown in Figure 2.3 for the Kit 1 offset short structure.

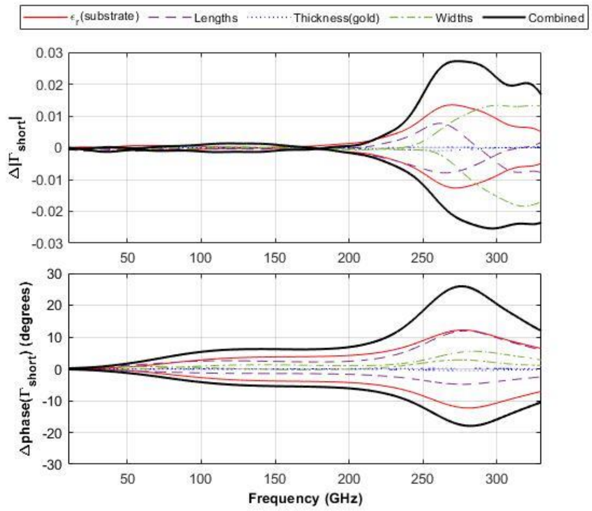

Fig 2.3: EM Simulation results for Kit 1 offset short device, depicting variations in device S-parameters resulting from structure parameter variations propagated through the EM simulations.

4.2.2 Calibration, verification and measurement techniques

RF probing is critical for accurate on-wafer measurements at sub-millimetre frequencies and requires precise alignment between the probe and the substrate. This involves probe planarization and a well-defined probe-to-substrate contacting approach. On-wafer measurements in sub-millimetre frequencies are significantly affected by probing accuracy, a result evident from a detailed study of conventional probing methods led by NPL.

For this reason, automated probing techniques were developed by VSL which facilitate reproducible and operator-insensitive probing uncertainties. A method was developed for automated RF probe landing using the RF-sensing principle. An investigation was performed on the correlation between probe-substrate distance and input reflection coefficient parameter in on-wafer measurements. The measurement results led to a better understanding of the interaction between various parameters involved in on-wafer probing and the development of an automated contact event detection algorithm. A series of broadband measurements collected with the proposed method and conventional manual probing showed about five times improved repeatability using the automated contacting technique, shown in Figure 2.4. Furthermore, VSL demonstrated probe-tip markings as suitable parameters for planarizing RF probes in on-wafer measurements and controlling the probe over travel distance. Probe tip marks with a standard deviation of 3 µm for probe tilt and 1 µm for overtravel distance have been achieved. These results were operator-independent and suitable for automated on-wafer measurements. These automated methods were embedded into a dedicated on-wafer measurement software program developed by VSL to support automated on-wafer measurements.

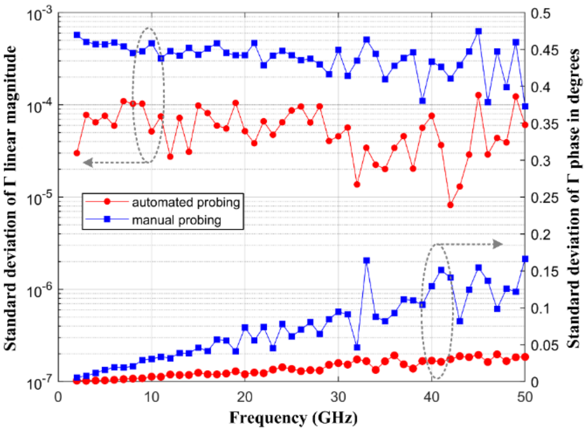

Fig 2.4: On-wafer probe contact repeatability estimates for manual and automated probe landing techniques.

PTB led an interlaboratory study involving three laboratories in the 140 to 220 GHz frequency band to determine suitable calibration techniques for millimetre-wave and THz VNA measurement systems. Different calibration approaches and measurement setups were used. Two laboratories applied off-wafer calibrations (TRL and SOLT), and one used multi-line TRL for on-wafer calibration. None of the DUTs acted as calibration standards. The study led to the following findings: Off-wafer TRL calibrations deliver inconsistent results, the SOLT calibration shows nonphysical ripples, and reliable results can only be obtained by on-wafer mTRL calibration. On-wafer multi-line TRL was identified as the best choice for the calibration of millimetre-wave and THz VNA measurement systems.

NPL led the development of the validation method for the measurement campaign. In terms of choice of verification device, six different types of devices, i.e., Load-Open, Open-Short, Load-Short, Attenuator, Filter, and Mismatched Line, were identified as the most appropriate devices for the verification technique. These devices have electrical characteristics that differ from typical calibration standards (i.e., Short-Short, Open-Open, Load-Load, 50 Ω lines) and therefore are ideal for verification. The first three devices are also part of 16-term calibration standards; however, they have not been used for calibration during measurement verification. These verification devices were included in both Kit 1 (for mm-wave bands) and Kit 2 (for THz bands). The table below gives a detailed list of these devices. Two types of ground configurations were designed for devices Load-Open, Open-Short, and Load-Short, to evaluate the impact of ground structures on the measurement results at high frequencies. A select group of verification standards were part of the interlaboratory comparison.

4.2.3 Uncertainty sources and uncertainty calculation

To work towards developing an uncertainty framework for CPW on-wafer measurements, PTB led a study into identifying the uncertainty sources that affect this type of measurement. Several types of on-wafer uncertainty sources stem from both external and internal disturbances. Internal effects, i.e., radiation and dispersion effects, originate from the physical nature of the transmission lines. To incorporate these disturbances, the uncertainty estimation has been revised to implement the new, improved CPW model developed by PTB. Figure 2.5 shows the uncertainty estimation of the characteristic impedance and propagation constants, including the new CPW model using the material and CPW dimensions of Kit 1. External effects, on the other hand, are caused by the influence of the microwave probe & neighbouring structures on the wafer, the propagation of parasitic modes (e.g surface waves and parallel plate modes) due to the measurement boundary condition, and radiation effects from the probes. It was found that certain calibration schemes, such as the TRL method, suffer from probe crosstalk errors. The influence of the thru standard in the mTRL calibration scheme was found to be particularly prone to probe coupling effects. Also, the impact of chuck boundary conditions in on-wafer measurements was investigated. With the benefit of these investigations, the layout of the calibration kits was optimized to mitigate the influence of these uncertainty sources as much as possible.

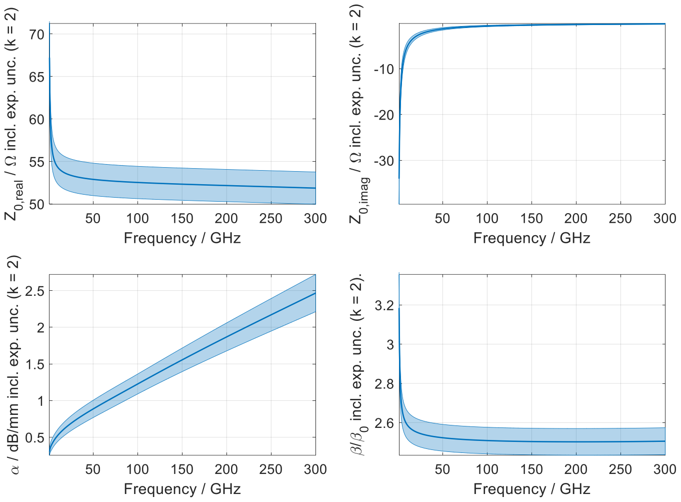

Fig 2.5: Estimates of uncertainty using nominal values of the CPW structure.

For sources of uncertainty that cannot be assessed experimentally, i.e. by measurements, electromagnetic simulation was used. VSL investigated the use of EM simulations for estimating uncertainties corresponding to the CPW devices up to 1.1 THz. The study improved the understanding of critical device parameters that predominantly affect the corresponding S-parameters. S-parameter uncertainties for all devices in Kit 1 and Kit 2 were estimated with the developed behaviour models. Furthermore, VSL and LNE also investigated the probe-related uncertainties, i.e. crosstalk, alignment and planarity offsets. The conventional uncertainty sources stemming from the VNA and RF cables were estimated according to the measurement-based techniques outlined in the EURAMET VNA guide for measurement uncertainties.

To calculate the uncertainty of the device-under-test (DUT), VSL developed a measurement model for co-variance-based uncertainty propagation in planar measurements, as shown in Figure 2.6. Each two-port network depicts a source of measurement uncertainty. The proposed method can support any number of uncertainty sources using the cascade of multiple two-port networks. In this example, uncertainty sources residing from the VNA, error terms, the frequency extenders and the probes were accounted for. The measurement model was fully integrated into the VNA calibration and uncertainty calculation software by VSL.

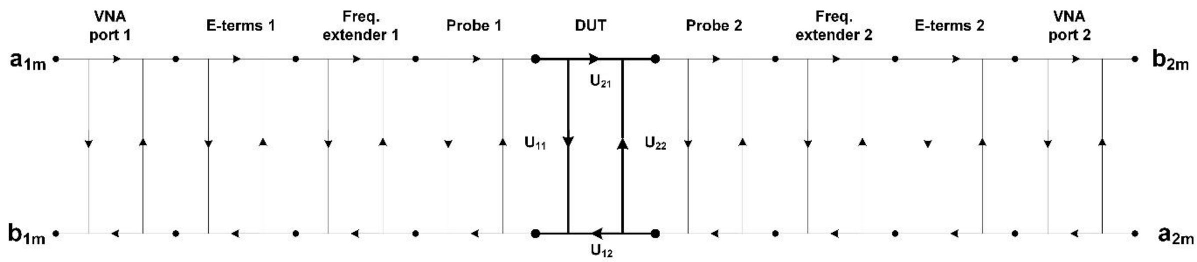

Fig 2.6: Measurement model for uncertainty propagation in on-wafer measurements.

4.2.4 Traceable calibration and verification measurements

NPL and LNE, with support from VSL, prepared a measurement protocol for the comparison campaign. Measurement results were submitted by NPL, PTB, FVB and Keysight for measurements up to 330 GHz and ULILLE, Chalmers and FormFactor contributed results up to 1.1 THz.

PTB evaluated combined uncertainty estimates up to 330 GHz using the comprehensive uncertainty budget developed in the PlanarCal project, including instrumentation errors, connector repeatability, and calibration standard uncertainties based on the use of an improved CPW model.

Furthermore, VSL estimated measurement uncertainties up to 1.1 THz and included reference standard uncertainties based on the CPW behaviour model employing electromagnetic (EM) simulations developed by VSL and also included probe cross-talk uncertainties estimated from the two-port structures comprising two one-port devices. VSL has embedded the co-variance-based uncertainty propagation method in their software for on-wafer calibration and uncertainty calculations. Both evaluation methods demonstrated uncertainties of a similar order of magnitude up to 330 GHz.

VSL collected and evaluated the measurement results for the comparison campaign up to 1.1 THz, and prepared a detailed measurement comparison report detailing the comparison results for the Kit 1 and Kit 2 structures. The excellent comparison results for Kit 1 agree strongly with the estimated measurement uncertainties (see Figure 2.7). PTB provided measurement-based expanded uncertainties for the frequency bands 110-170 GHz and 220-325 GHz. The difference between PTB and VSL uncertainty estimates is likely due to VSL not including other uncertainty sources residing from the VNA, frequency extenders, cables and connection repeatability. The measurement comparison for Kit 2 also shows fair agreement (again, see Figure 2.7). As only one laboratory conducted measurements from 500 GHz to 750 GHz, no comparison was possible for this frequency band. Most results show fair agreement with the calculated uncertainties for measurement results ranging from 330 - 500 GHz and 750 - 1100 GHz. The measurement uncertainties for Kit 2 were only estimated by VSL and again are based on simulated assessment. Furthermore, calibration accuracy above 750 GHz seemed to degrade and requires future investigation.

The successful completion of a first-of-a-kind international interlaboratory comparison in on-wafer measurements demonstrates the significant progress in extending traceability in on-wafer measurements up to 1.1 THz. VSL, with support from LNE, NPL, PTB, Chalmers, FormFactor, Keysight BE, FVB/FBH and ULILLE, have prepared a journal paper detailing the inter-laboratory comparison results, as shown in Figure 2.7, for on-wafer S-parameter measurements up to 1.1 THz. Furthermore, VSL, with support from LNE, NPL, PTB, Chalmers, FormFactor, Keysight BE, FVB/FBH and ULILLE, also prepared the report describing the techniques developed to support the extension of traceable planar S-parameter measurements to 1.1 THz. Therefore, objective 2 has been successfully achieved.

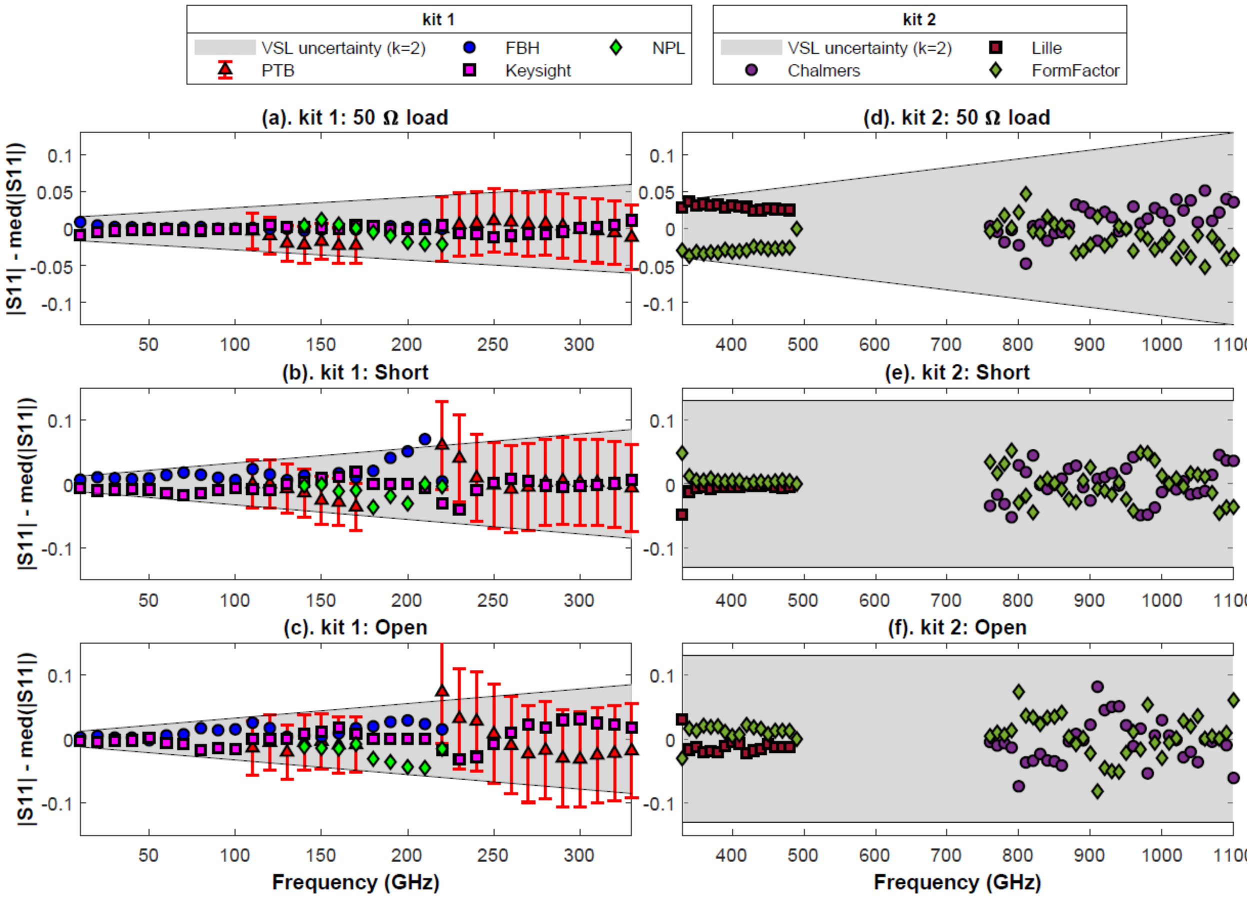

Fig 2.7: Comparison results for reflection coefficient measurements of one-port load, short, and open devices corresponding to kit 1 and kit 2.

4.3 Objective 3: To develop metrological traceability for power measurements in waveguide to 750 GHz. Two waveguide bands within this frequency range will be covered and these are 110 GHz to 170 GHz, and 500 GHz to 750 GHz.

The overall objective of this study was to establish traceable power measurements in two selected frequency bands using rectangular metallic waveguides within the frequency range from 110 GHz to 750 GHz. Specifically, waveguide calorimeters were developed, along with power sensor transfer standards and free-space measurements of power that were transferred to waveguide measurements. Interlaboratory measurements have been made in two waveguide bands, 110 GHz to 170 GHz and 500 GHz to 750 GHz, in order to validate these results.

4.3.1 Microcalorimeter measurements

In the framework of this project, the goal was to develop traceability for power measurement up to 170 GHz. Micro-calorimeter systems and transfer standards were developed for the 110 GHz to 170 GHz band and novel approaches for the calibration of RF power have been explored in three national metrology institutes (NMIs): NPL, LNE and PTB.

Fig 3.1: NPL microcalorimeter setup at D-Band.

Fig 3.2: LNE microcalorimeter setup at D-Band.

NPL established a new twin-line waveguide microcalorimeter system in D-band (from 110 to 170 GHz) to provide microwave power traceability for the measurement of effective efficiency of power sensors in this band (see Figure 3.1). The design of this microcalorimeter is optimized to operate with thermistor type thermoelectric sensors (TS), however, the TSs which were used for this study use a thermoelectric effect instead of a thermistor bead. The microcalorimeter was modified specially to accommodate this type of thermoelectric sensor.

LNE developed a twin-type microcalorimeter measurement setup (displayed in Figure 3.2) that is similar to the approach of the PTB setup and is used to calibrate D-Band thermoelectric TS from 110 to 170 GHz.

The measurement equipment developed by PTB consists of a new twin-line waveguide microcalorimeter system in D-band (from 110 to 170 GHz) (see Figure 3.3). The design was optimized to be suitable for thermistors and thermoelectric sensors. The thermoelectric power sensor was connected to a waveguide feed line, and a second waveguide was terminated by a dummy sensor of the same type, thus providing a symmetrical setup which is comparable to the NPL setup.

Fig 3.3: PTB microcalorimeter setup at D-Band.

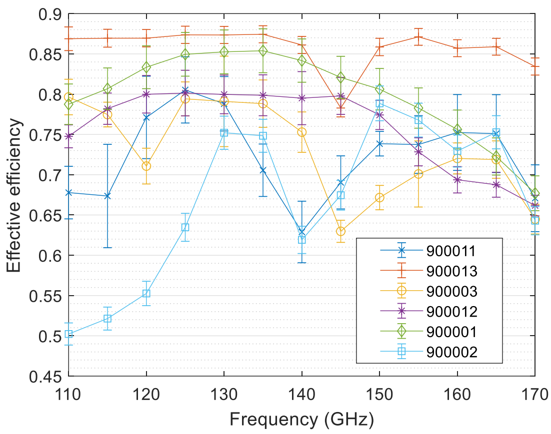

Fig 3.4: Effective efficiencies.

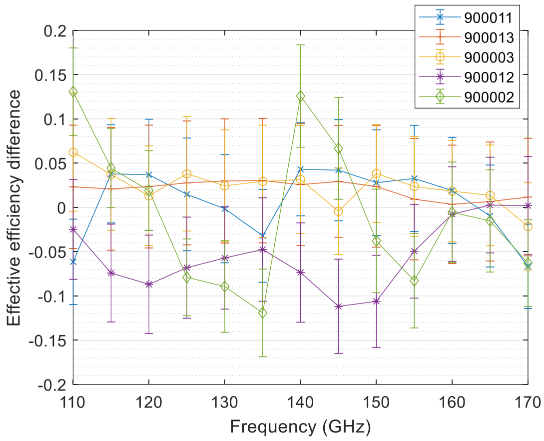

Fig 3.5: DCTMS deviation to the microcalorimeter measurements.

A selection of D-Band thermoelectric power sensors were characterized by NPL, PTB and LNE using each of their microcalorimeters from 110 to 170 GHz. The measured effective efficiencies varied between 0.629 to 0.874 and the uncertainties obtained ranged from 1.2% to 9.5%, depending on the measurement method and transfer standards used (compare Figures 3.4 and 3.5).

Finally, 95% of the difference between the DCTMS and microcalorimeter measurements of the laboratories is in the DCTMS uncertainty. This shows good agreement between the measurements from the three labs.

The second approach to power sensor characterisation involved a D-band thin-film bolometric power sensor, used for millimetre-wave metrology (Figure 3.6). The sensor has been characterized in a microcalorimeter and showed to have an effective efficiency of over 90%, whilst also demonstrating good reflection performance with a measured return loss of better than 15 dB across the entire D-band. The sensor achieved high power linearity between -10 dBm and +8 dBm and demonstrated a rise-and-fall time for the sensor response to RF power of better than 1.8 s. The measured frequency response of the sensor showed an efficiency that varies by less than 6% across the entire frequency band and produced a stable response after approximately 60 minutes.

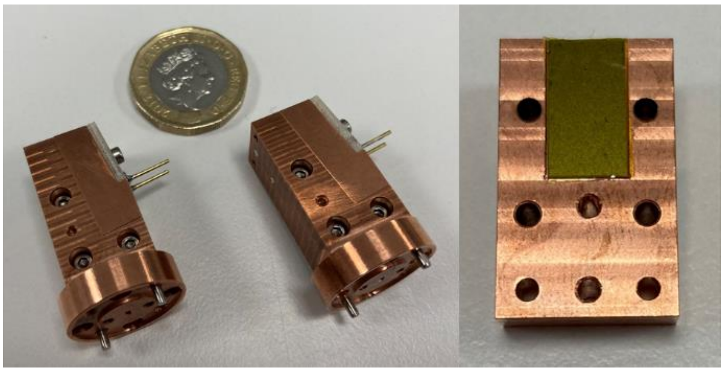

Fig 3.6: Fabricated thin-film bolometric power sensors. (a) Both sensors were assembled with the PCB and connectors attached. (b) Chip holder with the chip placed on the top.

4.3.2 Comparison of power measurements

The thermoelectric power sensor RS 900014 provided by PTB was circulated for a measurement comparison between TUBITAK UME, NPL and LNE. The DC heater of the thermoelectric power sensor malfunctioned during the NPL measurements. Therefore, NPL performed measurements with the DC heater at the first three frequencies and the other measurements were performed without the DC heater. 110 GHz was used as a reference frequency to calculate the generalized effective efficiency. Because of the referencing, NPL uncertainty was slightly larger than expected. LNE performed all the necessary measurements related to power but was unable to supply the final report due to equipment malfunction despite completing the power measurements.

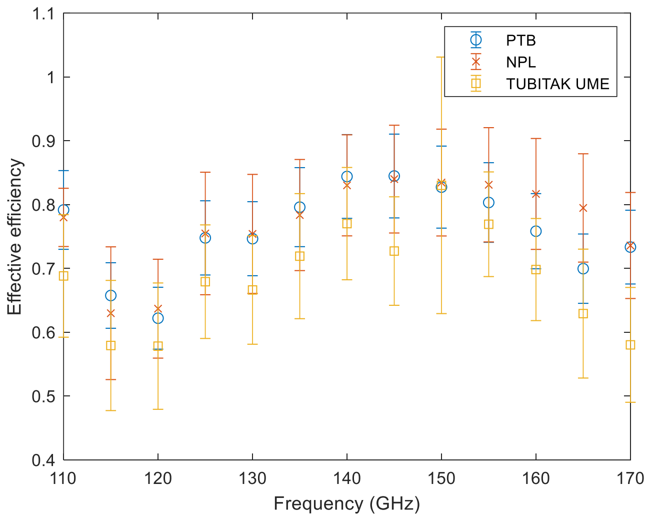

Fig 3.7: Effective efficiency results for the thermoelectric power sensor.

The effective efficiency and reflection coefficient of the thermoelectric power sensor were used to evaluate the participants' results. The calculated effective efficiency of TUBITAK UME and NPL are shown in Figure 3.7. PTB results were used to evaluate the thermoelectric power sensor behaviour. NPL and PTB measurements are traceable to their microcalorimeters. TUBITAK UME used a commercial power sensor/meter combination for the measurements.

PTB results were used to evaluate the participant's effective efficiency. The absolute difference for NPL was compared with the square root of the total of square uncertainties of NPL and PTB. The differences obtained were smaller for all frequencies except 165 GHz. The same method was also applied to the TUBITAK UME absolute differences, and smaller data was obtained for all frequency points except at 110, 145 and 170 GHz. Finally, 85% of the NPL and TUBITAK UME results were in good agreement with PTB results.

Furthermore, the calorimetric power sensor provided by TUBITAK UME was used with a WR 6.5 to WR 10 taper for D band (110 GHz – 170 GHz) power measurements and was measured by TUBITAK UME, NPL and LNE. The power applied to the calorimetric power sensor was measured by the participant's standard, and the power ratio between the measured power by the D-band calorimetric power sensor and the participant's power sensor was calculated.

TUBITAK UME, LNE and NPL calculated the power ratio using measured power from the D-band calorimetric power sensor and their own calorimetric power sensor. In addition, LNE measured the power using an R&S 170 TWG-type characterised thermoelectric power sensor and calculated the power ratio. LNE calculated the power ratio using two different data sources, one collected through the power meter's 'recorder' output and the other from the calorimetric power sensor's manufacturer software. The participants' power ratios are shown in Figure 3.8.

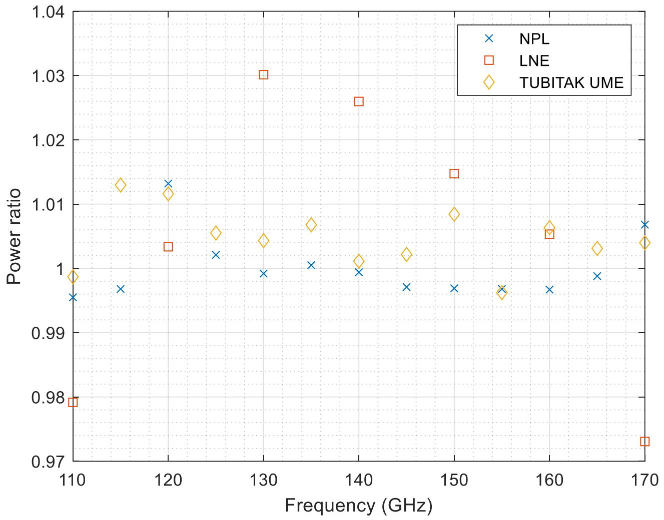

Fig 3.8: D-band calorimetric power sensor participants' power ratio.

In general, the power ratios are in excellent agreement with each other. This shows that the calorimetric power sensor had good stability whilst travelling between TUBITAK UME, NPL and LNE, and generates reproducible results.

The calorimetric power sensor used for the D-band measurements was also used for WM-380 band power measurements. To adapt the calorimetric power sensor to the WM-380 band, a WR-1.5 to WR-10 taper provided by VDI was attached.

TUBITAK UME, NPL, METAS, LNE and WAT in collaboration with GUM measured the power from the calorimetric power sensor/taper combination against their standard power measurement setup. Rough power ratios are shown in Figure 3.9 for the calorimetric power sensor, and the participants' standard power sensor was calculated. The power ratios were calculated using the measured powers from the standard and travelling power sensors and didn't apply corrections such as mismatch, losses, flange effects and ambient conditions. All these parameters are out of the scope of this work.

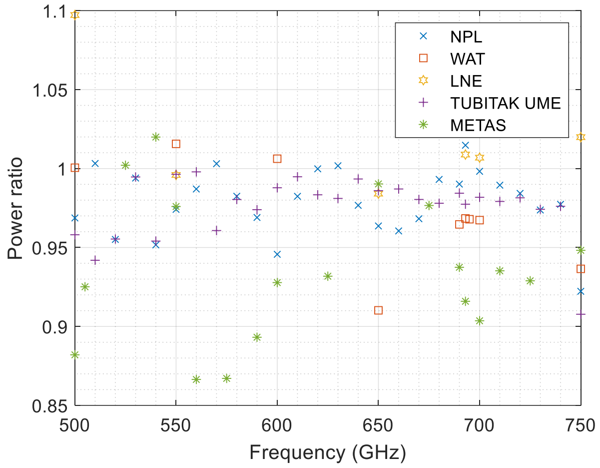

Fig 3.9: Participants' power ratios for the WM-380 band calorimetric power sensor.

All the participants except METAS used the same type of power sensor/taper combination as travelling calorimetric power sensor/taper combination. METAS used a pyroelectric power measurement setup. All measurements agree with each other, and deviations from the average are smaller than 12%, which was the given power uncertainty by METAS. Therefore, objective 3 has been successfully accomplished.

4.4 Objective 4: To develop metrological traceability for complex permittivity of dielectric materials to 750 GHz. Two waveguide bands will be covered and these are 140 GHz to 220 GHz, and 500 GHz to 750 GHz.

The overall objective of this study was to achieve traceable and accurate measurement and characterisation of materials properties (i.e. complex permittivity), at millimetre-wave and THz frequencies, for telecommunications and electronics technologies.

Specifically, this involved developing metrological traceability for the complex permittivity of dielectric materials at frequencies up to 750 GHz. Two waveguide bands were covered:140 to 220 GHz and 500 to 750 GHz. Various methods and setups i.e. VNA-based, resonant and optical-based, were utilised and were compared with each other in order to assess the reliability and utility of each method.

Each type of setup - resonant, VNA-based and optical - has been installed, tested and optimised successfully at GUM, METAS, NPL, LNE and WAT, as shown in Figure 4.1.

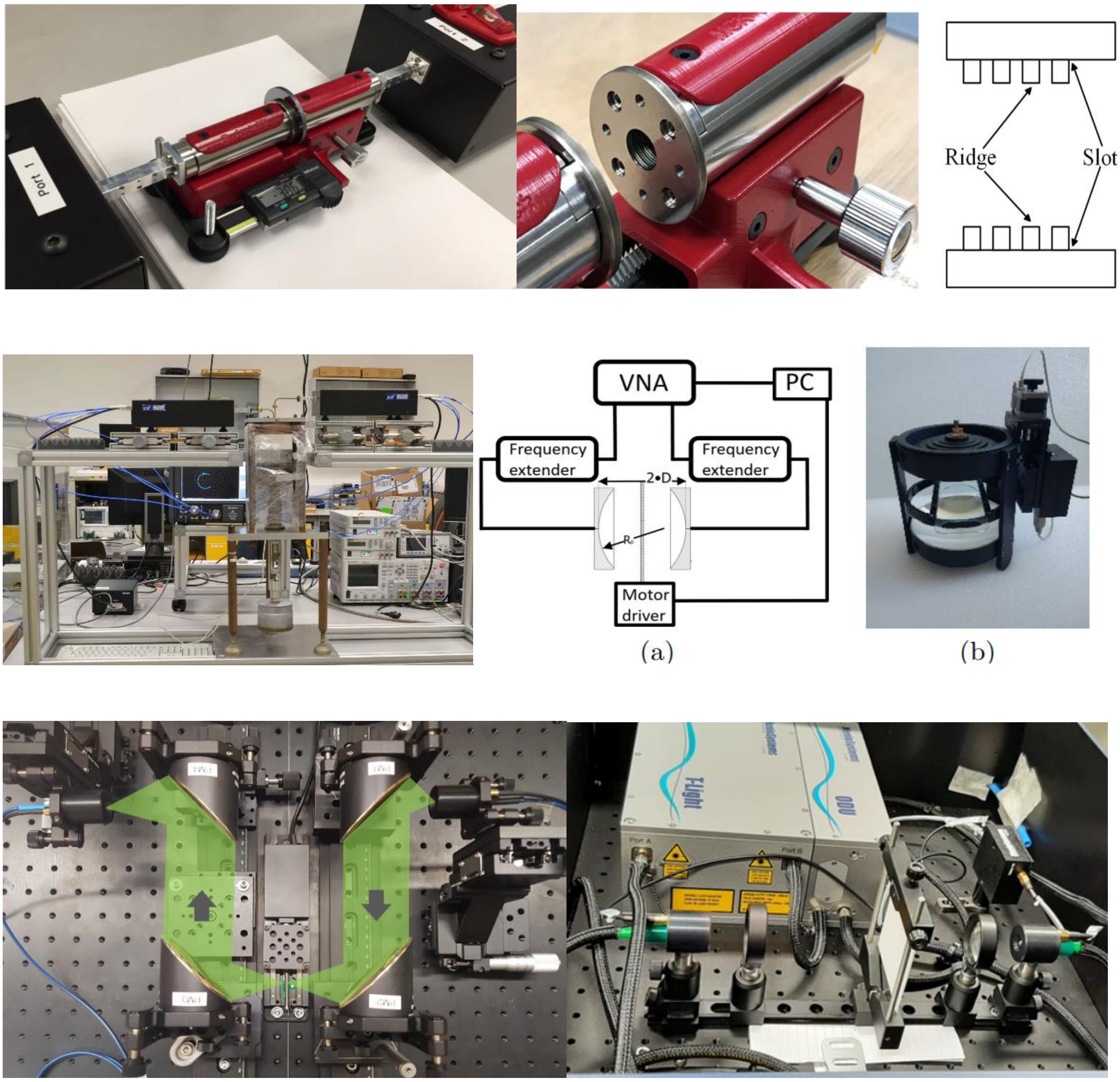

Fig 4.1: Schematic of VNA-based MCK (top), resonant (middle) and optical-based (bottom) setups.

Various calibration and extraction techniques were applied to the measurement systems. Different materials were measured and uncertainties were studied. CMI contributed to the extraction techniques and calculation of uncertainties for the VNA-based setups.

A guide for measurement parameter determination for optical setups, calibration procedures and material parameter extraction was prepared by METAS, NPL and LNE. NPL and METAS have also suggested new calibration methods and parameter-extraction techniques for the VNA-based MCK setups covering different WG frequency ranges.

4.4.1 VNA-based MCKs

These are novel, commercially available material characterization kits (MCK) provided by SWISSto12. These systems follow a "guided free-space" approach, using corrugated mode converters to provide a quasi-TEM mode in the air gap between two antennas. The mode converters are very compact, and measurements are easy to perform.

Systems were established in two frequency bands: 140 to 220 GHz (NPL) and 500 to 750 GHz (METAS). Improvements in the setups for better repeatability and for better control of sensitive parameters were investigated, e.g. positioning of the sample inside the MCK, and more accurate control and readout of slit width at the sample position.

The manufacturer of the MCK uses a relatively simple calibration technique, whereas better results should be achievable by using more advanced calibration techniques. Different choices of reference planes and calibration standards are available, which were compared with regard to feasibility and stability. The goal was to obtain reliable S-parameters at the location of material samples for further extraction of material parameters with the associated uncertainties.

4.4.2 Optical-based techniques

FDS (Frequency Domain Spectroscopy): This method requires a system installed with photomixers and two continuous wave (CW) lasers to generate and detect CW THz radiation. Traceability is established by measuring the optical frequencies of the two CW lasers with a reference wavemeter. Test measurements of different materials were performed to further improve the setup performance. METAS and NPL precisely defined how each spectrometer should be characterized. Both of these laboratories then successfully applied different methods for material parameter extraction.

TDS (Time Domain Spectroscopy): For these measurements, the different laboratories utilised different systems. NPL used a TeraFlash Pro spectrometer from Toptica Photonics set up in a standard optical configuration with four F/2 parabolic mirrors. The THz beam path was purged with dry air to eliminate absorption from atmospheric water vapour. Samples were placed in the collimated section of the beam, and laser alignment was used to ensure that they were positioned normal to the THz beam. The frequency resolution was 10 GHz. LNE used the TERA K15 THz Spectrometer from MenloSystems. This system incorporates a fibre-coupled configuration and is designed for operation with a laser with a beam diameter of around 1.5 µm. Its flexibility allows the THz path to be positioned outside the spectrometer housing if needed. WAT used the commercial TPS Spectra 3000 system from TeraView company. All measurements were conducted in the chamber with dry air. For the TDS method, the signal in the time domain was acquired. The frequency (f) is calculated by the firmware using Fourier transform. As a reference the empty setup was measured; subsequently, a measurement of the sample was performed in the same conditions.

4.4.3 Resonant Methods

Open-resonators are highly sensitive instruments that enable very precise measurement of the permittivity and loss from the measurement of Q-factor and resonant frequency. They can be used to measure very low losses, but are not generally suitable for measuring materials that have a high loss or are very thick. The aim was to characterise some low-loss materials (e.g. windows and substrates) at selected frequencies over a broad range by two laboratories, NPL and GUM. Two methods of using open resonators were compared; these are fixed length (resonant frequency is measured with and without a specimen) and variable length (the cavity is shortened to retune it when a specimen is inserted).

4.4.4 Comparison

Based on a pre-scheduled plan for the comparison project, all the participants completed their measurements. All participants reported their complete measurement results, whereas some also provided the associated measurement uncertainties. Several samples from various materials (low-loss, lossy, thick, thin etc.) have been measured. In addition to the original activity project partners (METAS, NPL, WAT, LNE, GUM), other partners also joined the EURAMET 1514 project (PTB, TUBITAK, UniFR).

Table 3: reference materials

Sample number	Name of material sample	# samples	Sample shape and size [mm]	Sample thickness [um] and uncertainty (2σ)
1	High-resistivity (HR) silicon	1	Ø 100	416.2 ± 2.2
2A1a	Fused silica, batch A	1	Ø 80	2068 ± 4
2A1b		1	Ø 80	2056 ± 8
2A2a		1	Ø 80	1016 ± 6
2A2b		1	Ø 80	1034 ± 4
2A3a		1	Ø 80	523 ± 10
2A3b		1	Ø 80	520 ± 8
2A4a		1	Ø 13	1968 ± 3
3	Borofloat	1	Ø 100	500.6 ± 0.1
4	TPX	1	Ø 100	6146.5 ± 16.4
5	YAG	1	Ø 60	2504 ± 8
6a	UHMW Polyethylene	1	Ø 80	1850 ± 40
6b		1	Ø 80	4967 ± 6
6c		1	Ø 13	1995 ± 22
6d		1	75 x 54	1815 ± 14
7a	Doped silicon	1	Ø 100	290.8 ± 0.9
7b		1	Ø 100	595.9 ± 3.4
8a	AF32 Schott	1	Ø 100	501 ± 1
8b		1	Ø 100	502 ± 3

	GUM OR	LNE TDS	METAS FDS	METAS MCK	NPL MCK	NPL OR	NPL TDS	PTB FS	PTB MCK	TUBITAK FS	UniFR TDE	WAT TDS
1	x	x	x	x	x		x		x	x	x	x
2A1a		x	x	x	x	x	x	x	x	x	x	
2A1b		x	x		x	x	x	x	x	x		
2A2a		x	x	x	x	x	x	x	x	x	x	
2A2b		x	x	x	x	x	x	x	x	x		
2A3a		x	x	x	x	x	x	x	x	x	x	
2A3b		x	x		x	x	x	x	x	x		
2A4a										x		x
3	x	x	x	x	x		x	x	x	x	x	x
4		x	x	x	x		x	x	x	x	x	x
5		x	x	x	x	x	x		x	x	x	x
6a	x	x	x	x	x	x	x	x	x	x	x	x
6b		x	x	x	x	x	x	x	x	x	x	
6c		x								x		x
6d		x		x	x	x	x	x	x	x		
7a		x	x	x	x		x			x	x	x
7b		x	x	x	x		x			x	x	x
8a	x	x	x	x	x		x	x	x	x	x	x
8b		x	x		x		x	x	x	x		x
9			x	x								

Fig 4.2: Comparison details: specification of the comparison samples (left); breakdown of samples measured by the participating labs (right).

The aim of this exercise was to provide a comprehensive comparison between different setups and different parameter-extraction techniques over a very wide frequency range. From the complex transmission data and the previously determined specimen thickness values, the material parameters have been extracted via different methods for all materials; this was to attain the complex refractive index and absorption coefficient, or alternatively, the real and imaginary part of permittivity. Results of the same batch of studied materials with different thicknesses (#2 Fused silica, #6 UHMW, #8 Schott-Glass) assisted with finding possible systematic errors in the calibration and extraction techniques, as well as the sensitivity, linearity and dynamic range/noise limits of each setup. For instance, the MCK measurements of Fused Silica samples (from the same batch, but with different thicknesses) show the reliability and consistency of the calibration techniques and the parameter-extraction methods (Figure 4.3).

4.4.5 Sample of Results

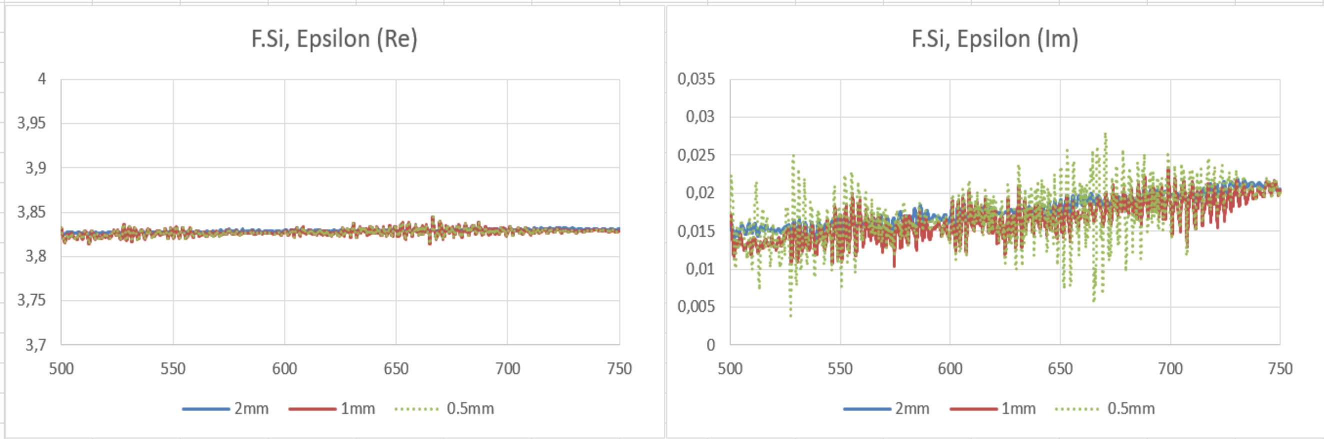

Fig 4.3: Measured dielectric constant (left: real component, right: imaginary component) of fused Silica with three different thicknesses .

In general, a good level of agreement was observed between different participants for many samples (Figures 4.4-4.6). However, for some materials such as doped silicon, or very low-loss samples like thin high-resistivity silicon and UHMW, the deviations are more visible. It is likely that improved results can be achieved by improving the calibration methods and adapting the parameter-extraction technique for each kind of sample. Objective 4 has been achieved successfully.

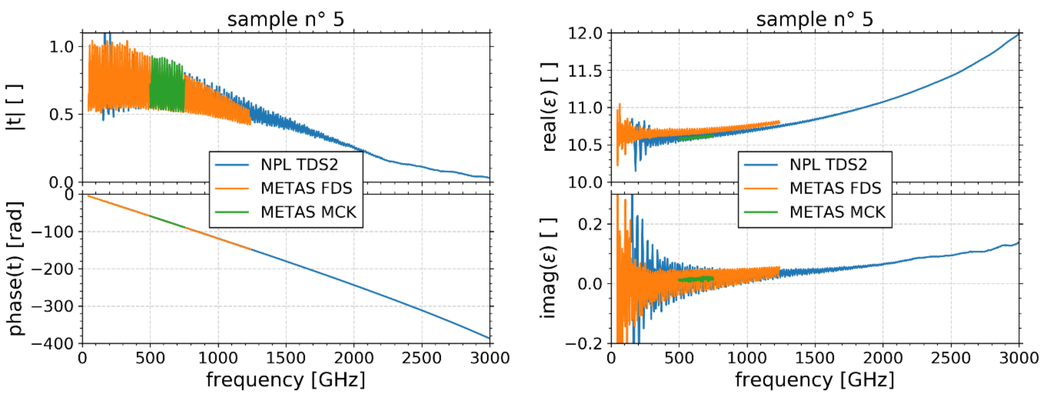

Fig 4.4: Measured magnitude and phase of the complex transmission (left) and extracted real and imaginary parts of the permittivity (right) for sample #5 (YAG, 2.5mm). NPL (Optical Time-Domain), METAS (Optical Frequency-Domain), and METAS VNA-based material characterization kit (MCK).

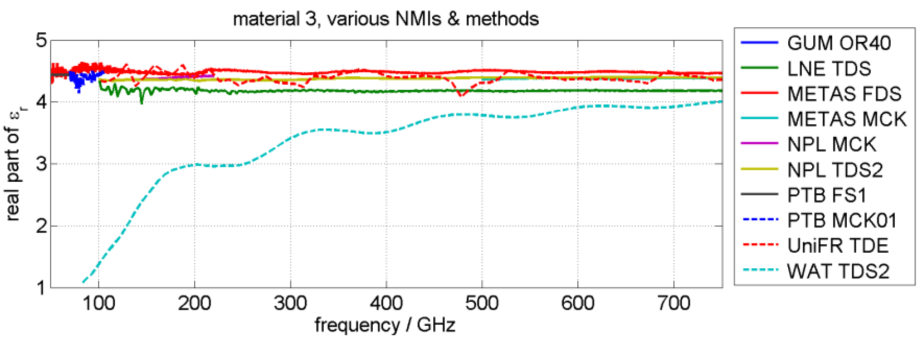

Fig 4.5: Borofloat Glass (0.5mm thickness), real-part of permittivity.

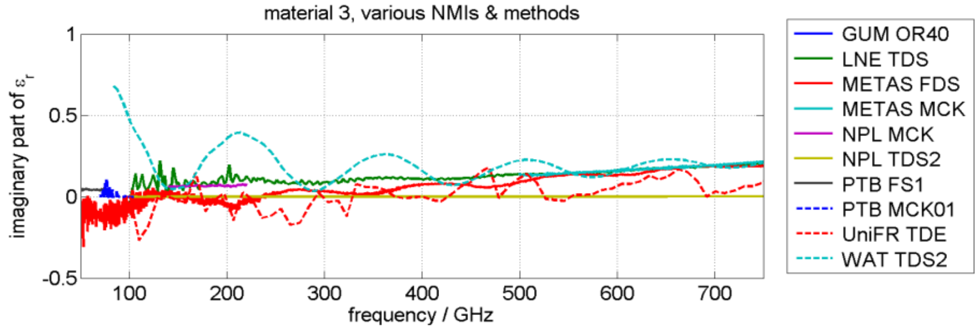

Fig 4.6: Borofloat Glass (0.5mm thickness), imaginary-part of permittivity.

5 Impact

Considerable efforts have been made to maximise the impact of this project within the European community of stakeholders and industrial end-users, and to ensure dissemination to, and uptake by, industry, academia, European and non-European National Metrology Institutes (NMIs) and standardisation bodies.

A range of activities have been undertaken to create impact from this project, and some highlights are described below.

- This project has produced 29 open access peer-reviewed scientific papers and technical reports, of which 14 are published in high impact journals including *Metrologia, IEEE Transactions on Instrumentation and Measurement*, *IEEE Transactions on Terahertz Science and Technology*, *IEEE Microwave and Wireless Components Letters*, *Journal of Infrared Millimeter and Terahertz Waves, Applied Sciences*, and *Metrolog*y. Additionally, 5 peer-reviewed papers have been accepted for presentation in major international conferences (i.e. 4 by CPEM 2022 and 1 by 99th ARFTG), 1 paper has been accepted for publication in *Journal of Infrared Millimeter and Terahertz Waves*, and 3 papers have been drafted/submitted to prestigious IEEE journals. In summary, research undertaken in this project has led to 36 peer-reviewed scientific papers, and among them 11 are joint publications.
- This project has been presented 25 times at conferences such as Conference on Precision Electromagnetic Measurements (CPEM), Microwave Measurement Symposium/Conference (ARFTG), IEEE International Microwave Symposium (IMS), International Conference on Electromagnetic Metrology (ICEM), IEEE International Conference on Smart Instrumentation, Measurement and Applications (ICSIMA), International Conference on Infrared, Millimeter, and Terahertz Waves (IRMMW-THz), International Conference on Electromagnetics in Advanced Applications (ICEAA), Asia-Pacific Microwave Conference (APMC), IEEE Workshop on Signal and Power Integrity (SPI), etc.
- Three one-day workshops have been held as part of premier international conferences: (i) One is entitled “Measurements at mmWave and Terahertz Frequencies of Three Measurement Quantities: S-Parameters, Power, and Complex Permittivity of Dielectric Materials”, at the European Microwave Week (EuMW) 2020; (ii) One is entitled “Research in Power and S-parameters Measurement at mmWave and Terahertz Frequencies”, at the EuMW 2021; and (iii) One is entitled “Recent developments in millimetre-wave measurement: S-parameters and material properties”, at the EuMW 2022. All these three workshops were about the outputs of this project, and the speakers were from either the consortium or its Technical Advisory Group (TAG).
- The consortium has also organised two training courses, one in July 2021 and the other one in July 2022. The training courses were held online, and each course included seven technical presentations covering all the technical work carried out under this project. Both courses were very successful, e.g. the first one was attended by more than 110 participants globally.

- This project has created a website for end users at http://projects.lne.eu/jrp-temmt/. Useful information such as publications and training course presentation slides has been made available on the website, which will exist beyond the lifetime of this project.
- Four teleconferences with the TAG have been held every nine months during the lifetime of this project. TAG members are a group of 16 experts in the project's scientific areas.
- An EURAMET pilot study entitled "Comparison on material parameter measurements in the THz spectral range with optical, resonant and VNA based setups" has been launched as part of this project. A comprehensive report has been produced based on this pilot study and published with open access on EURAMET's website.
- This project has provided inputs to a range of international standards committees including IEEE MTT/SCC P287, P2822, P1785, P3136; IEC TC46 and SC46F.

Impact on industrial and other user communities

This project enables accurate and traceable measurements of three key electrical quantities at millimetre-wave and THz frequencies. This will have a direct impact on communications and electronics industries exploiting this part of the spectrum. Notable examples include point-to-point backhaul for 5G communications, the IoT, radar sensors for CAVs, space-borne radiometers for Earth monitoring, and security imaging. Improvement of measurement accuracy and establishment of measurement traceability will enable manufacturers to provide confidence in their measurements and specifications.

This project has also significantly extended the measurement capabilities of the participating NMIs, to over 1 THz for S-parameter measurement and to 750 GHz for power and material measurement. This will lead to greatly improved access to, and dissemination of, measurement traceability for European accredited testing and calibration laboratories and manufacturers of test instrumentation. This will be beneficial for all end-users, including customers and suppliers of millimetre-wave and THz devices and systems.

The project has set up a Technical Advisory Group, formed of members from the end-user industry and metrology communities. Such direct interaction with industry ensures the project aligns with industrial needs and fosters knowledge transfer. The Technical Advisory Group currently comprises 15 end-users from the electronic, instrumentation, and semiconductor sectors, and 3 NMIs outside of Europe (AIST, Japan; NIM, China; and KRISS, Korea). Teleconferences with the Technical Advisory Group members were held in January 2020 at LNE (France) alongside the M9 project meeting, in October 2020 alongside the M18 project meeting, in July 2021 alongside with the M27 project meeting, and in July 2022 alongside the M39 project meeting.

Impact on the metrology and scientific communities

No single NMI currently has the capability to deliver this project, therefore, this project involved eight of Europe's NMIs and will synergise their national research programmes. During the project, preparatory tasks have been undertaken to subsequently establish a coordinated network of NMIs, including the NMI of Argentina (INTI), in order to provide a comprehensive measurement capability based on the outcomes of this project, and the previous EMRP project SIB62. This project has also fostered the development of three relatively small NMIs (CMI, GUM and TUBITAK) whose metrology programmes are at an early stage of development in the field of electrical measurements. This has been done through their working collaborations with the five experienced European NMIs (i.e. METAS, LNE, NPL, PTB and VSL) in this consortium. For example, the EURAMET comparison of material properties measured using different methods and different measurement setups involved four NMIs (i.e. GUM, LNE, METAS and NPL), and hence such activities have enhanced collaborations between these, and other, NMIs across Europe. The consortium has produced a proposal about a coordinated network of European NMIs that will provide comprehensive measurement capability at millimetre-wave and THz frequencies, developed a roadmap for the network, and submitted the report to EURAMET for consideration.

Impact on relevant standards

This project has so far provided inputs to seven standardisation bodies, i.e. **IEEE MTT/SCC P287** "Standard for Precision Coaxial Connectors (DC-110 GHz)"; **IEEE MTT/SCC P2822** "Recommended Practice for Microwave, Millimeter-wave and THz On-Wafer Calibrations, De-Embedding and Measurements"; **IEEE MTT/SCC P1785** "A New Standard for Waveguide Above 110 GHz"; **IEEE MTT/SCC P3136** "Universal Waveguide Interface for Frequencies of 60 GHz and Above"; **IEC/TC 46** "Cables, Wires, Waveguides, RF Connectors, RF and Microwave Passive Components and Accessories"; **IEC/SC 46F** "RF and Microwave Passive Components"; and **DKE/UK 412.4** "Passive RF and Microwave Components".

IEEE MTT/SCC P287 has recently published three standards, i.e. IEEE Std 287.1-2021, IEEE Std 287.2-2021, IEEE Std 287.3-2021, in which the E-band 1.35 mm coaxial connectors are included.

A EURAMET report document has also been produced regarding materials property measurements within the range of 110 GHz to 750 GHz. Additionally, the project results will be fed into other standardisation bodies such as the BIPM Key Comparison Database and the BIPM database of CMCs.

Longer-term economic, social and environmental impacts

The measurement science generated by this project will pave the way for the development of emerging applications including future telecommunications, autonomous vehicles, the IoT, and security imaging. This will enable European businesses to move into these areas and will support a strong competitive advantage. For established applications, e.g. measurement instruments and space radiometers, state of the art performance will ensure a commercial edge and allow European industry in these sectors to continue progress with key technologies and to attract business from global markets.

The social benefits of this project will be to retain a competitive advantage in Europe over worldwide competition on technology and thereby keep and grow expertise and much needed highly skilled electronic engineering and support staff jobs. This project also has a wider social impact on quality of life enabled by greater data transport in mobile networks, medical diagnostics using THz imaging, easier and safer mobility using CAV and security scanning in public places such as airports.

Space radiometers play a key role in Earth monitoring, which provides information about global climate change and weather forecasting. This project will facilitate more accurate and traceable measurements at millimetre-wave and THz frequencies, yielding radiometers with better performance. Improved energy efficiency of components and systems will also be supported by more accurate measurements, which will in turn support a reduction in energy consumption and should lead to a more sustainable environment.

Examples of user uptake

Outputs of this project have already been utilised by end-users in industry and academia, as shown below a few notable examples.

- Partner R&S has already implemented the new 1.35 mm E-band coaxial connector in two thermal power sensors, the R&S NRP90T and R&S NRP90TN. The work on establishing traceability for S-parameter measurements in E-band connectors has therefore become very relevant and timely. Other component manufacturers who are not part of the project consortium also benefit from the 1.35 mm E-band coaxial connector work in their designs of calibration standards.
- New measurement systems are now in place at several European NMIs (i.e. LNE, NPL and PTB) to enable both dimensional and electrical measurements to be made of coaxial components in the 1.35 mm line size. Next, these NMIs will work towards adding these capabilities as Calibration and Measurement Capability (CMC) entries in the BIPM key comparison database to provide metrological traceability for this new coaxial line size.
- Based on the outputs of this project, NPL is now preparing to launch on-wafer S-parameter measurements as a new measurement service. There has been no such service before this project at NPL. PTB is now extending the existing on-wafer calibration and measurement service to frequencies above 110 GHz.

NPL has developed the bespoke TRL calibration technique for the material characterisation kits (MCKs) with support from the manufacturer SWISSTO12. The manufacturer has been looking at including this new calibration method as one of the recommended default calibration methods.

6 List of publications

[1] R. Judaschke, M. Kehrt, and A. Steiger, "Comparison of Waveguide and Free-Space Power Measurement in the Millimeter-Wave Range", in *2019 44th International Conference on Infrared, Millimeter, and Terahertz Waves (IRMMW-THz)*, Paris, France, 1-6 Sept. 2019, pp. 1-2, https://oar.ptb.de/files/download/5e5d0f6f4c93903e3800394c

[2] A. Kazemipour, J. Hoffmann, D. Stalder, M. Wollensack, J. Rufenacht and M. Zeier, "THz Detector Calibration Based on Microwave Power Standards," in *2019 International Conference on*

Electromagnetics in Advanced Applications (ICEAA), 2019, pp. 0402-0403, https://doi.org/10.5281/zenodo.5771103

[3] A. Kazemipour, M. Wollensack, J. Hoffmann, S.K. Yee, J. Rufenacht, G. Gaumann, M. Hudlicka, M. Zeier, "Material Parameter Extraction in THz Domain, Simplifications and Sensitivity Analysis," in *2019 IEEE Asia-Pacific Microwave Conference (APMC)*, Singapore, Singapore, 10-13 Dec. 2019, pp. 276-278, https://doi.org/10.5281/zenodo.4243025

[4] G. N. Phung and U. Arz, "Parasitic Probe Effects in Measurements of Coplanar Waveguides with Narrow Ground Width," in *2020 IEEE 24th Workshop on Signal and Power Integrity (SPI)*, Cologne, Germany, 17-20 May 2020, pp. 1-4, https://oar.ptb.de/files/download/5f92a12a4c93902ba0000843

[5] A. Kazemipour, J. Hoffmann, M. Wollensack, D. Allal, M. Hudlicka, J. Ruefenacht, D. Stalder, M. Zeier, "VNA-Based Material Characterization in THz Domain without Classic Calibration and Time-Gating," in *2020 Conference on Precision Electromagnetic Measurements (CPEM)*, Denver (Aurora), CO, USA, 24-28 Aug. 2020, pp. 1-2, https://doi.org/10.5281/zenodo.4243044

[6] F. Mubarak, C. D. Martino, R. Toskovic, G. Rietveld and M. Spirito, "Automated Contacting of On-Wafer Devices for RF Testing," in *2020 Conference on Precision Electromagnetic Measurements (CPEM)*, Denver (Aurora), CO, USA, 24-28 Aug. 2020, pp. 1-2, https://zenodo.org/record/4276095

[7] Y. Wang, X. Shang, N. M. Ridler, T. Huang and W. Wu, "Characterization of Dielectric Materials at WR-15 Band (50–75 GHz) Using VNA-Based Technique," in *IEEE Transactions on Instrumentation and Measurement*, vol. 69, no. 7, pp. 4930-4939, July 2020, https://doi.org/10.1109/TIM.2019.2954010

[8] N. M. Ridler, S. Johny, X. Shang, W. Sun and A. Wilson, "Comparing Standardized and Manufacturers' Interfaces for Waveguides Used at Submillimeter Wavelengths," in *IEEE Transactions on Terahertz Science and Technology*, vol. 10, no. 5, pp. 453-459, Sept. 2020, https://doi.org/10.1109/TTHZ.2020.3010122

[9] Y. Wang, X. Shang, N. Ridler, M. Naftaly, A. Dimitriadis, T. Huang, W. Wu, "Material Measurements Using VNA-based Material Characterization Kits Subject to Thru-Reflect-Line Calibration," in *IEEE Transactions on Terahertz Science and Technology*, vol. 10, no. 5, pp. 466-473, Sept. 2020. https://doi.org/10.1109/TTHZ.2020.2999631

[10] A. Kazemipour, M. Wollensack, J. Hoffmann, M. Hudlička, S. K. Yee, J. Rüfenacht, D. Stalder, G. Gäumann, and M. Zeier, "Analytical Uncertainty Evaluation of Material Parameter Measurements at THz Frequencies", in *Journal of Infrared Millimeter and Terahertz Waves*, 41, pp. 1199–1217, 2020, https://doi.org/10.1007/s10762-020-00723-0

[11] N. Ridler, S. Johny, M. Salter, X. Shang, W. Sun, A. Wilson, "Establishing waveguide lines as primary standards for scattering parameter measurements at submillimetre wavelengths", in *Metrologia*, vol. 58, no. 1, 2021, https://doi.org/10.1088/1681-7575/abd371

[12] M. Naftaly and A. Gregory, "Terahertz and Microwave Optical Properties of Single-Crystal Quartz and Vitreous Silica and the Behavior of the Boson Peak," in *Applied Sciences*, vol. 11, no. 15, p. 6733, Jul. 2021, http://dx.doi.org/10.3390/app11156733

[13] M. Celep and D. Stokes, "Characterization of a Thermal Isolation Section of a Waveguide Microcalorimeter," in *IEEE Transactions on Instrumentation and Measurement*, vol. 70, pp. 1-7, 2021, Art no. 1008007, https://doi.org/10.1109/TIM.2021.3084306

[14] A. Kazemipour, J. Hoffmann, M. Wollensack, M. Hudlička, J. Rüfenacht, D. Stalder, D. Allal, G. Gäumann and M. Zeier, "Standard Load Method: A New Calibration Technique for Material Characterization at Terahertz Frequencies," in *IEEE Transactions on Instrumentation and Measurement*, vol. 70, pp. 1-10, 2021, Art no. 1007310, https://doi.org/10.1109/TIM.2021.3077660

[15] D. Ma, X. Shang, N. M. Ridler and W. Wu, "Assessing the Impact of Data Filtering Techniques on Material Characterization at Millimeter-Wave Frequencies," in *IEEE Transactions on Instrumentation and Measurement*, vol. 70, pp. 1-4, 2021, Art no. 6005904, https://doi.org/10.1109/TIM.2021.3067224

[16] G. N. Phung and U. Arz, "Anomalies in multiline-TRL-corrected measurements of short CPW lines," in *96th ARFTG Microwave Measurement Conference (ARFTG)*, San Diego, CA, USA, 18-22 January 2021, pp. 1-4, https://oar.ptb.de/files/download/6189062f8e2a000011003f89

[17] G. N. Phung and U. Arz, "Impact of Chuck Boundary Conditions on Wideband On-Wafer Measurements," in *IEEE 25th Workshop on Signal and Power Integrity (SPI)*, Siegen, Germany, 10-12 May 2021, pp. 1-4, https://oar.ptb.de/files/download/618907218e2a000011003f97

[18] A. Bystrov, Y. Wang, and P. Gardner. 2022. "Analysis of Vector Network Analyzer Thermal Drift Error" in *Metrology*, vol. 2, no. 2, pp. 150-160, 2022, https://doi.org/10.3390/metrology2020010

[19] M. Celep, M. Salek, D. Stokes, J. Skinner and Y. Wang, "Power Sensor Characterization From 110 to 170 GHz Using a Waveguide Calorimeter," in *IEEE Transactions on Instrumentation and Measurement*, vol. 71, pp. 1-7, 2022, Art no. 1002007, https://research.birmingham.ac.uk/en/publications/power-sensor-characterization-from-110-ghz-to-170-ghz-using-a-wav

[20] J. Krupka, B. Salski, T. Karpisz, P. Kopyt, L. Jensen and M. Wojciechowski, "Irradiated Silicon for Microwave and Millimeter Wave Applications," in *IEEE Microwave and Wireless Components Letters*, vol. 32, no. 6, pp. 700-703, June 2022, https://doi.org/10.1109/LMWC.2022.3161393

[21] M. Salek, M. Celep, T. Weimann, D. Stokes, X. Shang, G. N. Phung, K. Kuhlmann, J. Skinner, Y. Wang, "Design, Fabrication, and Characterization of a D-Band Bolometric Power Sensor," in *IEEE Transactions on Instrumentation and Measurement*, vol. 71, pp. 1-9, 2022, Art no. 8002509, https://research.birmingham.ac.uk/en/publications/design-fabrication-and-characterization-of-a-d-band-bolometric-po

[22] M. Celep, G. N. Phung, F. Ziadé, D. Stokes, J. Rühaak, K. Kuhlmann, D. Allal, "WG29/WR7 Band Thermoelectric Power Sensor Characterization using Microcalorimetry Technique", in *2022 IEEE/MTT-S International Microwave Symposium - IMS 2022*, 2022, pp. 876-879, https://doi.org/10.5281/zenodo.7303596

[23] T. Karpisz, B. Salski, P. Kopyt, J. Krupka and M. Wojciechowski, "Measurement of Uniaxially Anisotropic Dielectrics With a Fabry–Perot Open Resonator in the 20–50 GHz Range," in *IEEE Microwave and Wireless Components Letters*, vol. 32, no. 5, pp. 441-443, May 2022, https://doi.org/10.5281/zenodo.7071325

[24] G. N. Phung and U. Arz, "On the Influence of Thru- and Line-Length-Related Effects in CPW- Based Multiline TRL Calibrations," in *2021 97th ARFTG Microwave Measurement Conference (ARFTG), 2021*, pp. 1-4, https://doi.org/10.7795/EMPIR.18SIB09.CA.20220915A.

[25] G. N. Phung and U. Arz, "Parasitic Probe Effects in Measurements of Conductor-Backed Coplanar Waveguides," in *2021 Kleinheubach Conference*, 2021, pp. 1-4, https://doi.org/10.7795/EMPIR.18SIB09.CA.20220915B.

[26] G. N. Phung and U. Arz, "On the Influence of Metal Chucks in Wideband On-Wafer Measurements," *2022 98th ARFTG Microwave Measurement Conference (ARFTG)*, 2022, pp. 1-4, https://doi.org/10.7795/EMPIR.18SIB09.CA.20220915C.

[27] G. N. Phung, U. Arz and W. Heinrich, "Comparison of coplanar waveguide models at millimetre wave frequencies," *2022 IEEE 26th Workshop on Signal and Power Integrity (SPI)*, 2022, pp. 1-4, https://doi.org/10.7795/EMPIR.18SIB09.CA.20220915D

[28] J. Skinner, M. Salter, N. Ridler, Y. Wang, M. Salek, J. Stake, D. Jayasankar, J. Hesler, S. Durant, “Interlaboratory comparison of S-parameter measurements in WM-380 waveguide at frequencies from 500 GHz to 750 GHz,” NPL Report TQE 23, July 2022, https://doi.org/10.47120/npl.TQE23

[29] J. Skinner, M. Salter, N. Ridler, Y. Wang, M. Salek, J. Martens, J. Hesler, S. Durant, “Interlaboratory comparison of S-parameter measurements in WM-570 waveguide at frequencies from 325 GHz to 500 GHz,” NPL Report TQE 24, July 2022, https://doi.org/10.47120/npl.TQE24

This list is also available here: https://www.euramet.org/repository/research-publications-repository-link/

7 Contact details

N/A